Cell and Tissue Research (2019) 378:427–440
https://doi.org/10.1007/s00441-019-03070-2

REGULAR ARTICLE

Co-expression of C/EBPγ and ATF5 in mouse vomeronasal sensory neurons during early postnatal development

Haruo Nakano[1] · Yoshitaka Iida[1] · Takahiro Murase[1] · Natsuki Oyama[1] · Mariko Umemura[1] · Shigeru Takahashi[1] · Yuji Takahashi[1]

Received: 24 July 2018 / Accepted: 3 July 2019 / Published online: 16 July 2019

Abstract

The differentiation of sensory neurons involves gene expression changes induced by specific transcription factors. Vomeronasal sensory neurons (VSNs) in the mouse vomeronasal organ (VNO) consist of two major subpopulations of neurons expressing vomeronasal 1 receptor (V1r)/Gαi2 or vomeronasal 2 receptor (V2r)/Gαo, which differentiate from a common neural progenitor. We previously demonstrated that the differentiation and survival of VSNs were inhibited in ATF5 transcription factor-deficient mice (Nakano et al. Cell Tissue Res 363:621–633, 2016). These defects were more prominent in V2r/Gαo-type than in V1r/Gαi2-type VSNs; however, the molecular mechanisms responsible for the differentiation of V2r/Gαo-type VSNs by ATF5 remain unclear. To identify a cofactor involved in ATF5-regulated VSN differentiation, we investigated the expression and function of CCAAT/enhancer-binding protein gamma (C/EBPγ, Cebpg), which is a major C/EBP family member expressed in the mouse VNO and dimerizes with ATF5. The results obtained showed that C/EBPγ mRNAs and proteins were broadly expressed in the postmitotic VSNs of the neonatal VNO, and their expression decreased by the second postnatal week. The C/EBPγ protein was expressed in the nuclei of approximately 70% of VSNs in the neonatal VNO, and 20% of the total VSNs co-expressed C/EBPγ and ATF5 proteins. We examined the trans-acting effects of C/EBPγ and ATF5 on V2r transcription and found that the co-expression of C/EBPγ and ATF5, but not C/EBPγ or ATF5 alone, increased Vmn2r66 promoter reporter activity via the C/EBP:ATF response element (CARE) in Neuro2a cells. These results suggest the role of C/EBPγ on ATF5-regulated VSN differentiation in early postnatal development.

Keywords ATF5 · CEBPG · Vomeronasal sensory neurons · Differentiation · Mouse

Introduction

The vomeronasal organ (VNO) is one of the main sensory organs detecting pheromones and predator odors, which trigger and modulate sexual and social interactions in mammals (Liberles 2014). Vomeronasal sensory neurons (VSNs) in the VNO express two major subclasses of vomeronasal receptors, V1r and V2r, which are coupled to the G-proteins, Gαi2 and Gαo, respectively, and are located in the apical and basal vomeronasal epithelia (VNE), respectively (Dulac and Axel 1995; Jia and Halpern 1996; Herrada and Dulac 1997; Matsunami and Buck 1997; Ryba and Tirindelli 1997). V1r/Gαi2- and V2r/Gαo-type VSNs are derived from common neural progenitors and precursors with the sequential expression of Mash1, Ngn1, and NeuroD1 (Cau et al. 1997; Murray et al. 2003), which give rise to immature neurons that express GAP43, β-tubulin III, and doublecortin (DCX) and ultimately differentiate into mature OMP-positive VSNs with the expression of V1r or V2r (Enomoto et al. 2011; Oboti et al. 2015). The transcription factors, Bcl11b and Tfap2e, are expressed in VSNs to promote V2r/Gαo-type VSN differentiation (Enomoto et al. 2011; Lin et al. 2018); however, the molecular mechanisms responsible for the differentiation of V1r/Gαi2- and V2r/Gαo-type VSNs remain unclear.

We previously examined the effects of a deficiency in activating transcription factor 5 (ATF5) in VSNs using ATF5-deficient ($ATF5^{-/-}$) mice and demonstrated that the

Electronic supplementary material The online version of this article (https://doi.org/10.1007/s00441-019-03070-2) contains supplementary material, which is available to authorized users.

✉ Haruo Nakano
haruo@toyaku.ac.jp

[1] Laboratory of Environmental Molecular Physiology, School of Life Sciences, Tokyo University of Pharmacy and Life Sciences, 1432-1 Horinouchi, Hachioji, Tokyo 192-0392, Japan

differentiation of VSNs was inhibited at the stage of maturation in association with apoptosis (Nakano et al. 2016). The expression of a series of V1r and V2r genes was significantly decreased in the ATF5$^{-/-}$ VNO, indicating that the ATF5 deficiency affected V1r/Gαi2- and V2r/Gαo-type VSNs. However, the defect was more severe in V2r/Gαo-type than in V1r/Gαi2-type VSNs: OMP expression was normal in V1r/Gαi2-type, but not in V2r/Gαo-type VSNs, and apoptotic cells were frequently localized in the basal layer of the VNE, suggesting the critical role of ATF5 in the maturation and survival of V2r/Gαo-type VSNs (Nakano et al. 2016). ATF5 controls cell differentiation and survival in other cell types including olfactory sensory neurons, pancreatic β-cells, and adipocytes (Wang et al. 2012; Zhao et al. 2014; Juliana et al. 2017), in part by the physical interaction with a CCAAT/enhancer binding protein (C/EBP) transcription factor (Zhao et al. 2014). To identify a cofactor involved in ATF5-regulated VSN differentiation, we investigated the expression and function of C/EBPγ in VSNs. C/EBPγ is a small C/EBP family member that has a C-terminal bZIP DNA-binding domain but lacks a transactivation domain (Cooper et al. 1995). C/EBPγ dimerizes with ATF5 via the bZIP domain with higher affinity among C/EBP family members (Nishizawa and Nagata 1992; Vinson et al. 1993; Newman and Keating 2003). Furthermore, C/EBPγ mRNAs are strongly expressed in the sensory neuron layer of the main olfactory epithelium (MOE) and VNO in mouse embryos (Allen Brain Atlas: http://developingmouse.brain-map.org/gene/show/12396). Here, we demonstrated that C/EBPγ mRNAs and proteins were broadly expressed in the immature and early mature VSNs of the early postnatal VNO, and 20% of the VSNs co-expressed C/EBPγ and ATF5 in their nuclei. We also found that the co-expression of C/EBPγ and ATF5 increased V2r promoter reporter activity in mouse neuroblastoma. These

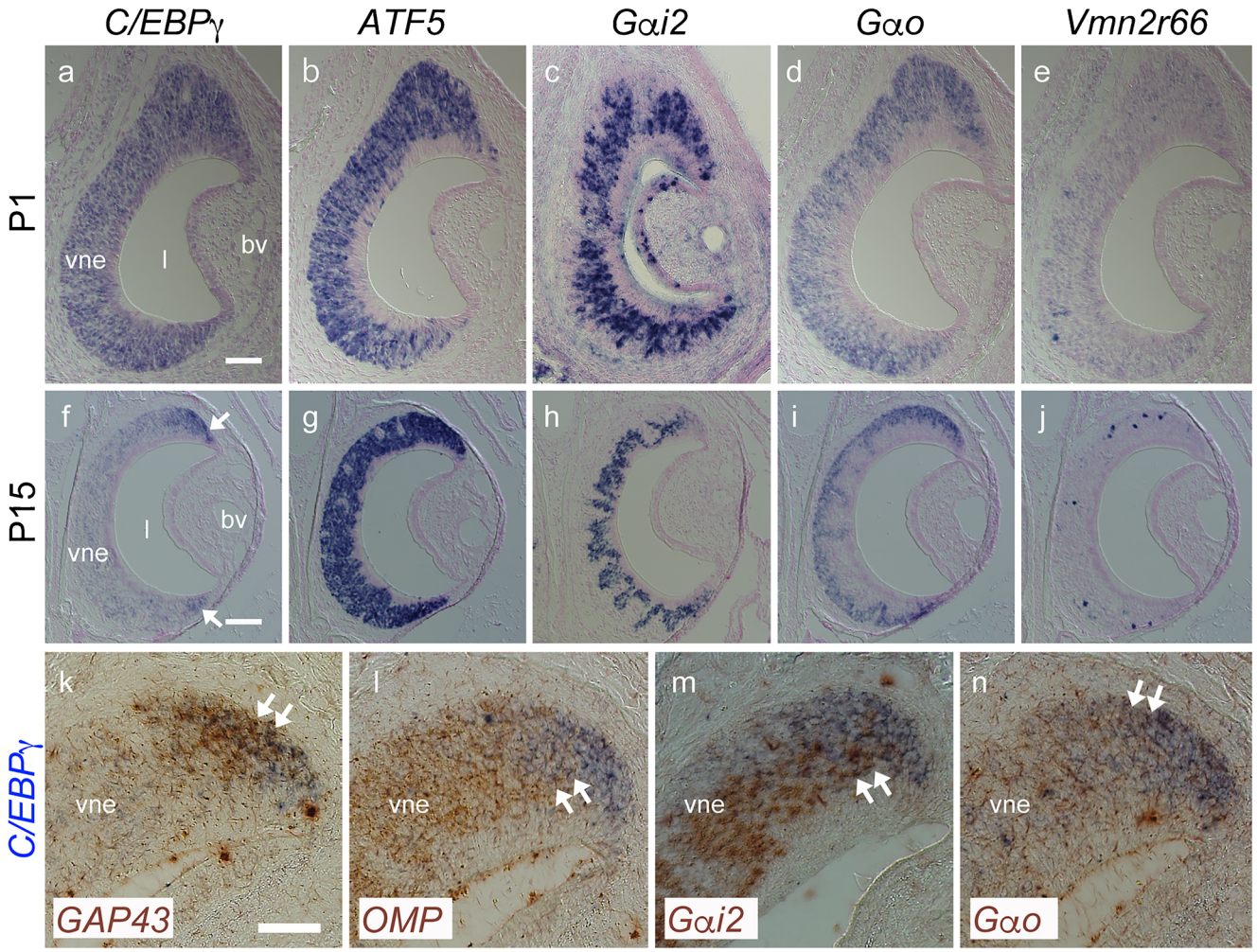

Fig. 1 C/EBPγ mRNA expression in the mouse vomeronasal epithelium. **a**–**j** In situ hybridization with RNA probes to *C/EBPγ* (**a**, **f**), *ATF5* (**b**, **g**), *Gαi2* (**c**, **h**), *Gαo* (**d**, **i**), and *Vmn2r66* (**e**, **j**) on coronal sections of the vomeronasal organ at P1 (**a**–**e**) and P15 (**f**–**j**). Arrows in **f** indicate *C/EBPγ*-positive cells at the marginal region of the vomeronasal epithelium. **k**–**n** Double in situ hybridization for *C/EBPγ* (purple) combined with *GAP43* (**k**), *OMP* (**l**), *Gαi2* (**m**), or *Gαo* (**n**) in brown at the marginal region of the vomeronasal epithelium (P15). Double arrows indicate the overlapping expression of the marked genes. bv blood vessel, l lumen, vne vomeronasal epithelium. Scale bars indicate 50 μm (**a**, **k**) or 100 μm (**f**)

results indicate that C/EBPγ is expressed in VSNs and associates with ATF5 to drive the maturation of VSNs in early postnatal development.

Materials and methods

Mice

C57/BL6 mice were maintained and mated to obtain pups at the animal facility at Tokyo University of Pharmacy and Life Sciences under specific pathogen-free conditions. ATF5-deficient ($ATF5^{-/-}$) mice were generated as previously described (Umemura et al. 2015). $ATF5^{+/-}$ mice were maintained with a C57/BL6 background and were mated to generate $ATF5^{+/+}$ and $ATF5^{-/-}$ pups for analyses. The day of birth was designated as postnatal day (P) 0. All mouse studies were approved by the Institutional Animal Experiment Committee of the university and were performed in accordance with institutional and governmental guidelines.

In situ hybridization

All mice were sacrificed by cervical dislocation. The snouts and nasal cavities of pups (P0–P15) were fixed in 4% paraformaldehyde (PFA) in phosphate-buffered saline (PBS) at 4 °C overnight. Snouts and nasal cavities at P15 were then immersed in 0.5 M EDTA solution to decalcify at 4 °C for at least 24 h. After washes with PBS, samples were cryoprotected in 20% sucrose in PBS, embedded in Tissue-Tek OCT compound, and cryosectioned. Coronal sections (thickness of 10 μm) were collected on PLATINUM adhesive coat glass slides (Matsunami, Osaka, Japan) and stored at − 80 °C until used.

In situ hybridization using digoxigenin (DIG)- and fluorescein (FITC)-labeled RNA probes was performed as previously described (Simmons et al. 2008; Nakano et al. 2016). Briefly, sections on slides were fixed in 4% PFA/PBS, washed with PBS, incubated with proteinase K (15 μg/ml, 10 min), re-fixed with 4% PFA/PBS, acetylated (0.25% acetic anhydride in 0.1 M triethanol amine, pH 8.0), and hybridized with DIG-labeled probes at 65 °C overnight (for double in situ hybridization, FITC-labeled probes were also added at this stage and hybridized at 60 or 65 °C). Hybridization buffer contained 1× salts (200 mM NaCl, 13 mM Tris, 5 mM sodium phosphate monobasic, 5 mM sodium phosphate dibasic, and 5 mM EDTA, pH 8.0), 50% formamide, 10% (*w*/*v*) dextran sulfate, 1 mg/ml yeast tRNA, 1× Denhardt's solution (WAKO, Osaka, Japan), and a cRNA probe. Posthybridization washes were followed by a RNase A treatment (400 mM NaCl, 10 mM Tris (pH 7.5), 5 mM EDTA, and 20 μg/ml RNase A) at 37 °C for 30 min. After blocking with 0.05 M maleic acid buffer containing 2% blocking reagent (Roche Diagnostics, Mannheim, Germany), 20% normal sheep serum, and 0.1% Tween 20, sections were incubated with an anti-DIG antibody (Roche Diagnostics) in blocking solution (1:1000 or 1:2500 dilution) at 4 °C overnight. After further washing, signals were visualized using 4-nitroblue tetrazolium chloride (NBT)/5-bromo-4-chloro-3-indolyl-phosphate (BCIP) as a substrate. In double in situ hybridization, the anti-DIG antibody conjugated to alkaline phosphatase was inactivated at 65 °C in maleic acid buffer for 30 min, followed by 30 min in 0.1 M glycine (pH 2.2). Sections were blocked again for 1 h and incubated overnight with an anti-FITC antibody (1:500 or 1:1000; Roche) at 4 °C. After washing, color was developed using INT/BCIP (Roche) until a brown precipitate was visible. In single NBT/BCIP coloring, slides were counterstained with Nuclear Fast Red, dehydrated, cleared in xylene, and mounted in Entellan (Merck Millipore, Darmstadt, Germany). In in situ hybridization containing brown INT/BCIP precipitates, sections were mounted with aqueous mounting medium (Dako, Glostrup, Denmark). Tissue sections were viewed under a microscope (BX50, Olympus, Tokyo, Japan) equipped with a charge-coupled device (CCD) camera (VB-6010, Keyence, Osaka, Japan). Probes were prepared from the cDNA of *C/EBPγ* (*Cebpg*) (nucleotides 264-738, NCBI reference sequence NM_009884), *Atf5* (nucleotides 299-1150, GenBank accession number AF375475), *Gαi2* (*Gnai2*) (nucleotides 252-1195, NCBI reference sequence NM_ 008138), *Gαo* (*Gnao1*) (nucleotides 816-1694, NCBI reference sequence

Table 1 The number of C/EBPγ single-, ATF5 single-, or C/EBPγ and ATF5 double-positive VSNs in the vomeronasal epithelium (VNE) with postnatal ages

Age	Total VSNs	C/EBPγ	ATF5	C/EBPγ and ATF5
P0	658 ± 121	348 ± 88 (52.9%)	59 ± 30 (9.0%)	122 ± 29 (18.5%)
P7	1043 ± 82	557 ± 77 (53.4%)	53 ± 16 (5.1%)	226 ± 77 (21.7%)
P15	1338 ± 26	64 ± 13 (4.8%)	18 ± 3 (1.3%)	35 ± 11 (2.6%)
P21	1142 ± 59	90 ± 17 (7.9%)	16 ± 5 (1.4%)	23 ± 9 (2.0%)
P32	1155 ± 115	139 ± 65 (12.1%)	17 ± 12 (1.5%)	16 ± 9 (1.4%)

The number of immunopositive cells in the entire region of the VNE without the supporting layer was counted and averaged in three or four tissue sections per mouse (positive cells/tissue section). Values represent the mean ± standard deviation (SD) of three mice. Values in parentheses indicate the mean proportion of positive/total cells (%)

NM_010308), *Vmn2r66* (nucleotides 1236-2046, NCBI reference sequence NM_001033878), *GAP43* (nucleotides 219-1210, NCBI reference sequence NM_008083), and *OMP* (nucleotides 4-641, NCBI reference sequence NM_011010). cDNA was generated by RT-PCR, cloned into pGEM-3zf (+) or pBluescript KS (+), and verified by sequencing.

Immunofluorescence

The dissected snouts and nasal cavities of pups (P0–P32) were fixed in 4% PFA in PBS at 4 °C for 3–4 h. Snouts at P15–P32 were then immersed in 0.5 M EDTA solution to decalcify at 4 °C for at least 24 h. After rinses with PBS, nose samples were cryoprotected in 20% sucrose in PBS and embedded in Tissue-Tek OCT compound. Coronal cryosections were prepared to obtain VNO. Tissue sections on the slides were blocked with PBS containing 3% bovine serum albumin (BSA) and 0.3% Triton X-100 at room temperature for 1 h. In some experiments, normal donkey serum (5%) was used instead of BSA for blocking. After blocking, an incubation with the primary antibody in PBS containing 1% BSA, 0.1% Triton X-100, and 0.05% NaN_3 (1% BSA/PBST) was performed at 4 °C overnight. The following primary antibodies and dilutions were used: goat anti-ATF5 (1:400, sc-46934, Santa Cruz, Dallas, TX, USA), goat anti-OMP (1:2,000, 019-22291, WAKO, Osaka, Japan), rabbit anti-C/EBPγ (1:300, HPA120124, Sigma-Aldrich, St. Louis, MI, USA), and goat anti-DCX (1:300, sc-8066, Santa Cruz). Regarding double labeling, two primary antibodies were incubated together. After three washes with PBS, sections were incubated with the secondary antibody in 1% BSA/PBST at room temperature for 2 h. The following secondary antibodies were used at a 1:200 or 1:400 dilution: Alexa 488-conjugated anti-goat IgG (Thermo Fisher Scientific, Invitrogen, Waltham, MA, USA), CFL 488-conjugated anti-goat IgG (Santa Cruz), and CFL 555-conjugated anti-rabbit IgG (Santa Cruz). Nuclei were stained with Hoechst 33342 (final concentration 5 μg/ml). After washes with PBS, tissue sections on slides were mounted using fluorescent mounting medium (Dako) and viewed under a fluorescent microscope equipped with a CCD camera (Biorevo, BZ-9000, Keyence).

To quantify C/EBPγ, ATF5, DCX, and OMP immunoreactivities and co-labeling in VSNs, thin cryosections (thickness of 10 μm) were prepared as described above, and every 15th section (150-μm increments) was processed for C/EBPγ, ATF5, DCX, and OMP immunofluorescences. The number of immunopositive cells and total VSNs (Hoechst staining) in the entire region of the VNE without the supporting layer were counted using Photoshop and ImageJ software and averaged in three or four VNO sections per mouse. Data represent the average ± standard deviation (SD) of three mice.

qRT-PCR

The VNO was dissected out from postnatal pups (P0 and P14-P15, $ATF5^{+/+}$ and $ATF5^{-/-}$ genotypes) and then homogenized in ISOGEN II reagent (Nippon Gene, Tokyo, Japan). Total RNA was prepared, and first-strand cDNA was then synthesized using ReverTra Ace reverse transcriptase (TOYOBO, Osaka, Japan) according to the manufacturer's instructions. Real-time RT-PCR was performed using the real-time PCR system Rotor-Gene Q (Qiagen, Venlo, the Netherlands) with KAPA SYBR FAST qPCR reagent (Nippon Genetics, Tokyo, Japan) according to the manufacturer's instructions. Data were normalized by β-actin expression and expressed as relative values against the wild type ($ATF5^{+/+}$). Statistical analyses were performed using the Student's unpaired *t* test. $P < 0.05$ indicated a significant difference. The following primers were used for detection: C/EBPγ (Cebpg)-F: TAGTGACGAATACCGCCAGC, C/EBPγ (Cebpg)-R: GTGCGCATGCTCAAGAAACA, Gαi2 (Gnai2)-F: AGTACCGTGCCGTGGTCTAC, Gαi2 (Gnai2)-R: ATGACACCGGACAGGTCTTC, Meis2-F: TAGTGACG AATACCGCCAGC, Meis2-R: GTGCGCATGCTCAA GAAACA, Gαo (Gnao1)-F: GTCACCGACATCATCATTGC, Gαo (Gnao1)-R: AGGTTAGACAGGGGCTTGGT, Tfap2e-F: TTGCAGGCGATAGATGACCC, Tfap2e-R: CGGAGCAG AAGACCTCACTG, Vmn1r8-F: GCCTATCCCACAGT TACCCC, Vmn1r8-R: TACACACTTGCCACAGCACA, Vmn1r42-F: CCCAGGAGGGATGGGTGATA, Vmn1r42-R: CCTGTGCCCACGAATGAACT, Vmn2r28-F: GCAAGGTC ATGGTTGCTGTAG, Vmn2r28-R: TGGTAGGTATGTAC CAATTTCTCA, Vmn2r66-F: CCTTGCTTTACATTGGTCAT CCC, Vmn2r66-R: TTCTTCTTCCTGGAACAGTAGCC, β-actin-F: ATGGAATCCTGTGGCATCCATG, and β-actin-R: CCACACAGAGTACTTGCGCTCA.

In silico analysis of the CARE on V2r promoters

The C/EBP:ATF response element (CARE, TGATGCAAT) was searched for in the promoter region of intact 191 V1r

Fig. 2 C/EBPγ protein expression in the mouse vomeronasal epithelium. ▶ **a**–**c** Immunofluorescence of C/EBPγ (green) on vomeronasal organs at P0 (**a**), P7 (**b**), and P15 (**c**). Nuclear Hoechst staining (magenta) is merged. Arrows in **a**–**c** indicate C/EBPγ-positive cells in the vomeronasal epithelium. **d**–**k** C/EBPγ-positive cells were characterized using double immunofluorescence for C/EBPγ (red) combined with doublecortin (DCX) or OMP (green) on the vomeronasal epithelium at P0: DCX (**d**–**g**) and OMP (**h**–**k**). Images (**e**–**g**) and (**i**–**k**) are at a higher magnification of the square region in **d** and **h**, respectively. Arrowheads in **e**–**g** and **i**–**k** indicate double-positive VSNs for the marked genes. **l**–**m** Double immunofluorescence of C/EBPγ (red) with DCX or OMP (green) on the vomeronasal epithelium at P15. Arrows in **l** and **m** indicate DCX/C/EBPγ- and OMP/C/EBPγ-positive VSNs, respectively. Scale bars indicate 50 μm. **n** The percentage of DCX- (closed bar) or OMP-positive cells (open bar) among C/EBPγ-positive VSNs in the vomeronasal epithelium at P0, P7, P15, and P21. Data represent the average ± SD of three mice

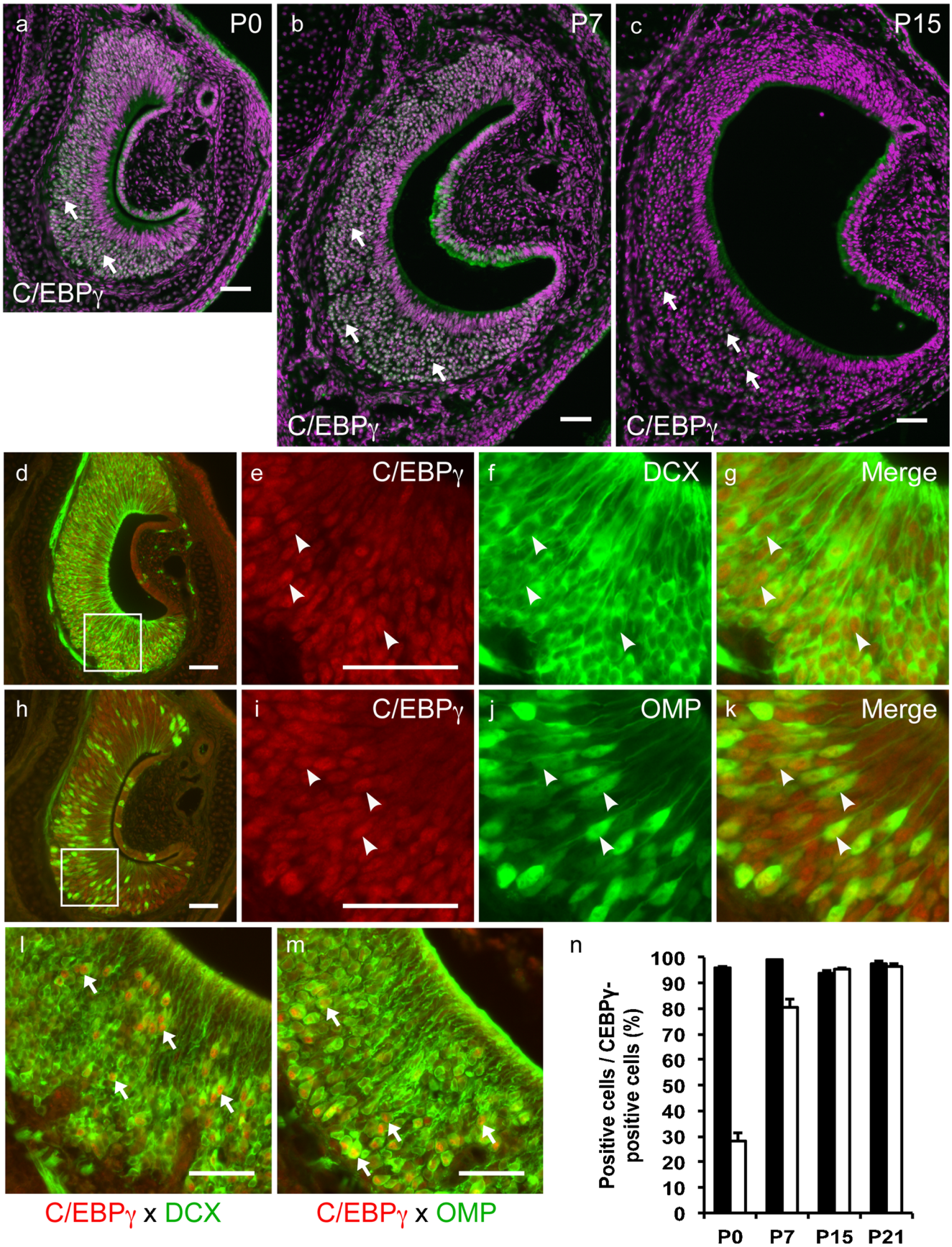
a
P0
C/EBPγ
b
P7
C/EBPγ
c
P15
C/EBPγ
d
e
C/EBPγ
f
DCX
g
Merge
h
i
C/EBPγ
j
OMP
k
Merge
l
m
C/EBPγ x DCX
C/EBPγ x OMP
n
Positive cells / CEBPγ-positive cells (%)
100
90
80
70
60
50
40
30
20
10
0
P0
P7
P15
P21

and 121 V2r genes using the JASPAR algorithm (http://jaspar.genereg.net; Khan et al. 2018). Since the transcriptional start sites (TSS) of many V1r and V2r genes have not yet been defined, the sequence of the region 2 kb upstream of the 5′ end of the 5′UTR or CDS of 191 V1r and 121 V2r genes was retrieved from the UCSC genome browser database (mouse GRCm38/mm10) and scanned for the CARE (TGATGCAAT) using the ATF4-binding profile (ID: MA0833.1) in JASPAR with the default setting.

Expression vectors and promoter reporters

Mouse ATF5 cDNA in pBlueScript (Shimizu et al. 2009) was subcloned into the pcDNA3.1(+) expression vector (Thermo Fisher Scientific, Invitrogen). C/EBPγ cDNA was amplified by PCR from mouse neonatal nose cDNA and cloned into the EcoR-I and Xba-I sites in pcDNA3.1(+). The following primers were used. C/EBPγ CDS Fw: CGGAATTCCGGTGT TGGCAAAGGAACGTG, Rev.: GCTCTAGAGCACTG CCCTGGGTTATCAGAA. The upstream region of the Vmn2r66 gene (1420 bp: − 1251 to + 169) was amplified by PCR from mouse genomic DNA and inserted into the pGL3 basic vector (Promega, Madison, WI, USA) using Mlu-I/Bgl-II in the multi-cloning site immediately upstream of the start codon of *Firefly* luciferase. The following primers were used: pVmn2r66-Luc1 Fw: GGGACGCGTGCTGCCTACAA AATTCCATCA, Rev: GGGAGATCTTTTTGTGAACC CATCCAGGT. The TSS of *Vmn2r66* mRNA was inferred from the RNA sequencing data of the mouse VNO (Ibarra-Soria et al. 2014). We performed 5′-RACE cloning of *Vmn2r66* mRNA from P15 VNO, and obtained the clone with a 5′end corresponding to the site near the TSS (+ 16 bp from TSS).

A deletion of the pVmn2r66-Luc1 construct was prepared using PCR with the following forward primers: pVmn2r66-Luc2: GGGACGCGTTTATAGTAAGAATTTTCACTC, pVmn2r66-Luc3: GGGACGCGTAATATCTACAA ATACTGGGGA, and pVmn2r66-Luc4: GGGACGCG TTGAGTTCAGTTGGAGTCATTGG, and the pVmn2r66-Luc1 reverse primer, as described above. A mutation in the CARE site (− 176 to − 168: TGATGTAAT) in the Vmn2r66 promoter region was introduced into pVmn2r66-Luc4 as GACGCGTCT using PCR with the following primers: pVmn2r66-Luc4mut Fw: CGACGCGT*C*TCTG AGGTAACTGTTTCAAAT and Rev: GTATTCCA AATGAGTTTTACTAGAAATTAT.

Promoter reporter luciferase assay

Mouse neuroblastoma Neuro2a cells were maintained in Dulbecco's modified Eagle's medium (Nissui, Japan), supplemented with 10% fetal bovine serum (FBS, Thermo Fisher Scientific, Gibco) and 2 mM L-glutamine (Thermo Fisher Scientific, Invitrogen) at 37 °C in an atmosphere of 5% CO_2. On the day of transfection, Neuro2a cells were plated at 5×10^4 cells in 0.5 ml with 24-well formats and co-transfected with 100 ng of pGL3 *Firefly* luciferase reporter vectors, 20 ng of the pRL-SV40 *Renilla* luciferase control vector (Promega), and 200 ng of pcDNA3.1 expression vectors using Fugene 6 (Promega). *Firefly* and *Renilla* luciferase activities were measured consecutively using the Dual-Luciferase Reporter Assay System (GLOMAX 20/20 LUMINOMETER, Promega) 48 h after transfection. Reporter luciferase activities were normalized to each *Renilla* luciferase activity and expressed as relative values against the parental vector (pcDNA). All experiments were conducted in triplicate and repeated at least twice on different days. All values are the average ± SD calculated from the results of triplicates in two or three independent experiments. The Student's unpaired *t* test to compare pcDNA and C/EBPγ+ATF5 or one-way ANOVA followed by a post hoc test (Tukey-Kramer) to compare four treatments (pcDNA, C/EBPγ, ATF5 and C/EBPγ+ATF5) was performed. $P < 0.05$ indicated a significant difference.

Results

In situ hybridization data has demonstrated that *C/EBPγ* mRNAs are strongly expressed in the embryonic MOE and VNE in mice (Allen Brain Atlas: http://developingmouse.brain-map.org/gene/show/12396). We examined the expression of *C/EBPγ* mRNA in the VNE at the neonatal stage (P0 or P1) and found that *C/EBPγ* mRNA was broadly expressed in VSNs of the VNE (Fig. 1a). *ATF5* as well as *C/EBPγ* mRNA displayed a broad expression pattern in the VNE (Fig. 1b). At this stage, *Gαi2* is mainly expressed in the apical region of the VNE (Fig. 1c), while *Gαo* is broadly expressed in both the apical and basal regions of the VNE, as previously described (Fig. 1d; Enomoto et al. 2011). *Vmn2r66* (a V2r pheromone receptor) mRNA was detected in a few VSNs at the basal VNE (Fig. 1e). We then examined the expression of *C/EBPγ* mRNA on P15 when V1r/Gαi2- and V2r/Gαo-type VSNs had fully separated into the apical and basal layers of the VNE, respectively (Prince et al. 2013). At this stage, the expression of *C/EBPγ* mRNAs was concentrated in the marginal region of the VNE (Fig. 1f, arrows). In contrast,

Fig. 3 Co-expression of C/EBPγ and ATF5 in vomeronasal sensory neurons. (a–e‴) Double immunofluorescence of C/EBPγ (a) and ATF5 (b) with nuclear Hoechst staining (c) on the vomeronasal epithelium at P0. Fluorescent images were merged in (d). (e–e‴) Images are at a higher magnification of the square region in (a–d). Arrows in (e–e‴) indicate C/EBPγ and ATF5 double-positive VSNs. (f–k) Double immunofluorescence of C/EBPγ (f, i, red) and ATF5 (g, j, green) and merged images (h, k) on the vomeronasal epithelium at P7 (f–h) and P21 (i–k). Arrows indicate C/EBPγ and ATF5 double-positive VSNs. Scale bars indicate 50 μm (a, f, i) and 25 μm (e)

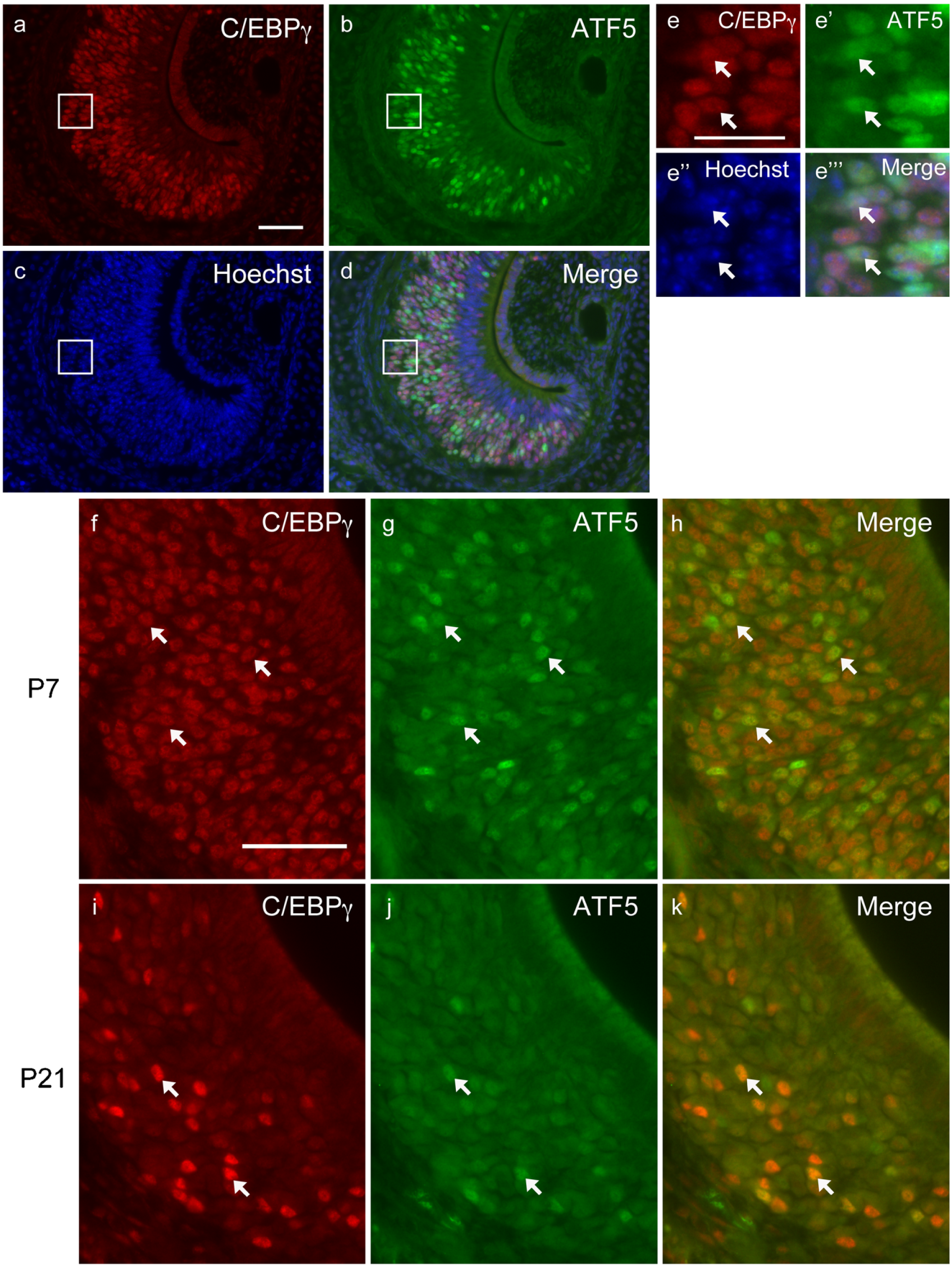
a
C/EBPγ
b
ATF5
c
Hoechst
d
Merge
e
C/EBPγ
e'
ATF5
e''
Hoechst
e'''
Merge
P7
f
C/EBPγ
g
ATF5
h
Merge
P21
i
C/EBPγ
j
ATF5
k
Merge

ATF5 mRNA was still expressed throughout the entire VNE (Fig. 1g), similar to the neonatal stage. We confirmed that the expression of *Gαi2* and *Gαo* was localized to the apical and basal layers of the VNE, respectively (Fig. 1h, i). Furthermore, *Vmn2r66*-positive VSNs were frequently observed at the basal layer of the VNE (Fig. 1j). To characterize *C/EBPγ*-positive cells in the marginal region of the VNE at P15, we performed the double in situ hybridization of *C/EBPγ* combined with *GAP43* (immature VSN marker) or *OMP* (mature VSN marker). We found that *C/EBPγ* and *GAP43* signals overlapped in the VSNs of the marginal region (Fig. 1k, double arrows). *OMP* expression was mainly detected in the central region of the VNE, and its signal partially overlapped with the *C/EBPγ* signal (Fig. 1l, double arrows). The strong overlapping between *C/EBPγ* and *GAP43* signals but not OMP ones was also observed in the basal olfactory sensory neuron layers of the MOE (Supplemental Fig. S1). We also performed the double in situ hybridization of *C/EBPγ* combined with *Gαi2* (apical VSN marker) or *Gαo* (basal VSN marker) and found the co-expression of *C/EBPγ* with *Gαi2* and *Gαo* in the VSNs of the marginal region (Fig. 1m, n, double arrows). These results indicated that *C/EBPγ*-positive cells in the marginal region largely corresponded to immature V1r/Gαi2- and V2r/Gαo-type VSNs. To examine C/EBPγ protein expression in VSNs, we performed an immunofluorescence study with a commercial anti-C/EBPγ antibody. The anti-C/EBPγ antibody specifically detected the murine C/EBPγ protein (16.4 kDa) in Neuro2a cell lysates with the overexpression of C/EBPγ in a Western blot analysis (Supplementary Fig. S2). Consistent with in situ hybridization results, C/EBPγ proteins were ubiquitously expressed in the nuclei of approximately 70% of the VSNs (71.4%, $n = 3$; Table 1) of the VNE at the neonatal stage (Fig. 2a, arrows). C/EBPγ-positive VSNs remained broadly distributed in the VNE at P7 (Fig. 2b, arrows) but drastically decreased to approximately 7% at P15 (7.4%, $n = 3$; Table 1) and were sparsely observed in the VNE without the localization at the marginal region (Fig. 2c, arrows). C/EBPγ-positive cells constituted 10–14% of the VSNs at P21 (9.9%, $n = 3$) and P32 (13.5%, $n = 3$; Table 1). To characterize C/EBPγ-positive VSNs in the VNE, we performed the double immunofluorescence of anti-C/EBPγ with either anti-DCX (immature and early mature VSNs; Oboti et al. 2015) or anti-OMP (mature VSNs). DCX was ubiquitously expressed in the VSNs of the VNE at P0 (Fig. 2d, green), and more than 90% of C/EBPγ-positive VSNs co-expressed DCX (Fig. 2e–g, arrowheads and n). In contrast, approximately 30% of C/EBPγ-positive VSNs (28.1 ± 3.0%, $n = 3$; Fig. 2n) were co-labeled with OMP (Fig. 2 h and i–k, arrowheads). VSNs that co-expressed C/EBPγ and OMP increased to 80% of C/EBPγ-positive cells at P7 (80.6 ± 2.9%, $n = 3$; Fig. 2n). At P15 and P21, over 90% of C/EBPγ-positive VSNs co-expressed DCX and OMP in the VNE (Fig. 2 l, m, arrows and n). These results indicate that C/EBPγ mRNAs and proteins were broadly expressed in the VSNs of the VNO at the neonatal stage; however, their expression drastically decreased by the second postnatal week. Double immunofluorescence demonstrated that C/EBPγ-expressing cells corresponded to immature and mature VSNs in the VNE.

To examine the relationship between C/EBPγ and ATF5 expression in the postnatal VNO, we performed double immunofluorescence with anti-C/EBPγ and anti-ATF5 on VNO sections at P0 (Fig. 3a–d) and found that the C/EBPγ protein was co-expressed with the ATF5 protein in the nuclei of VSNs (Fig. 3e–e‴, arrows). We noted that the intensities of the nuclear C/EBPγ and ATF5 signals varied in VSNs; however, there was no correlation between C/EBPγ and ATF5 signal intensities in individual VSNs (data not shown). We counted the numbers of C/EBPγ single-, ATF5 single-, and C/EBPγ and ATF5 double-positive VSNs in VNO sections at P0 and found that approximately 20% of the total VSNs expressed both C/EBPγ and ATF5 (18.5%, $n = 3$; Table 1), while approximately 50% and 10% of the VSNs expressed C/EBPγ (52.9%, $n = 3$) or ATF5 alone (9.0%, $n = 3$; Table 1), respectively. The co-expression of C/EBPγ and ATF5 was still found in approximately 20% of the VSNs of the VNE at P7 (21.7%, $n = 3$; Table 1; Fig. 3f–h, arrows). We observed a small portion of VSNs co-expressed C/EBPγ and ATF5 in the VNE at P15 (2.6%, $n = 3$), P21 (2.0%, $n = 3$; Fig. 3i–k, arrows), and P32 (1.4%, $n = 3$; Table 1).

To examine the effects of the ATF5 deficiency on *C/EBPγ* expression in VSNs, we performed in situ hybridization with the *C/EBPγ* probe on wild-type ($ATF5^{+/+}$) and ATF5-deficient ($ATF5^{-/-}$) VNO sections at P0. The results obtained showed that the expression of *C/EBPγ* in VSNs was similar between $ATF5^{+/+}$ and $ATF5^{-/-}$ VNOs (Fig. 4a, b). A quantitative PCR (qPCR) analysis with *C/EBPγ* mRNA demonstrated that the expression of *C/EBPγ* in the $ATF5^{-/-}$ VNO was similar to that in the wild-type VNO at P0 (Fig. 4c). We also examined the expression of apical-VSN marker (*Gnai2* and *Meis2*), basal-VSN marker (*Gnao1* and *Tfap2e*), and vomeronasal receptor genes (*Vmn1r8*, *Vmn1r42*, *Vmn2r28*, and *Vmn2r66*) and found that only the expression of *Vmn1r8* was significantly decreased in the $ATF5^{-/-}$ VNO at this stage (Fig. 4c). We extended the qPCR analysis with wild-type and $ATF5^{-/-}$ VNOs at P14–P15 and found that the expression of *C/EBPγ* was significantly reduced in the $ATF5^{-/-}$ VNO than in the

Fig. 4 C/EBPγ expression in the ATF5-deficient vomeronasal epithelium. **a**, **b** In situ hybridization of the *C/EBPγ* probe on $ATF5^{+/+}$ (**a**) and $ATF5^{-/-}$ (**b**) vomeronasal epithelia at P0. The scale bar indicates 50 μm. **c**, **d** Quantitative PCR analysis on the expression of *C/EBPγ*, apical-VSN marker (*Gnai2* and *Meis2*), basal-VSN marker (*Gnao1* and *Tfap2e*), and vomeronasal receptor genes (*Vmn1r8*, *Vmn1r42*, *Vmn2r28*, and *Vmn2r66*) in $ATF5^{+/+}$ (closed bar) and $ATF5^{-/-}$ (open bar) vomeronasal epithelia at P0 (**c**) and P14-P15 (**d**). Results were normalized by the expression of $ATF5^{+/+}$ types and represent the average ± SD of six (P0) and three (P14–P15) different animals. The Student's unpaired *t* test was performed to compare the $ATF5^{+/+}$ and $ATF5^{-/-}$ types (*$P < 0.05$)

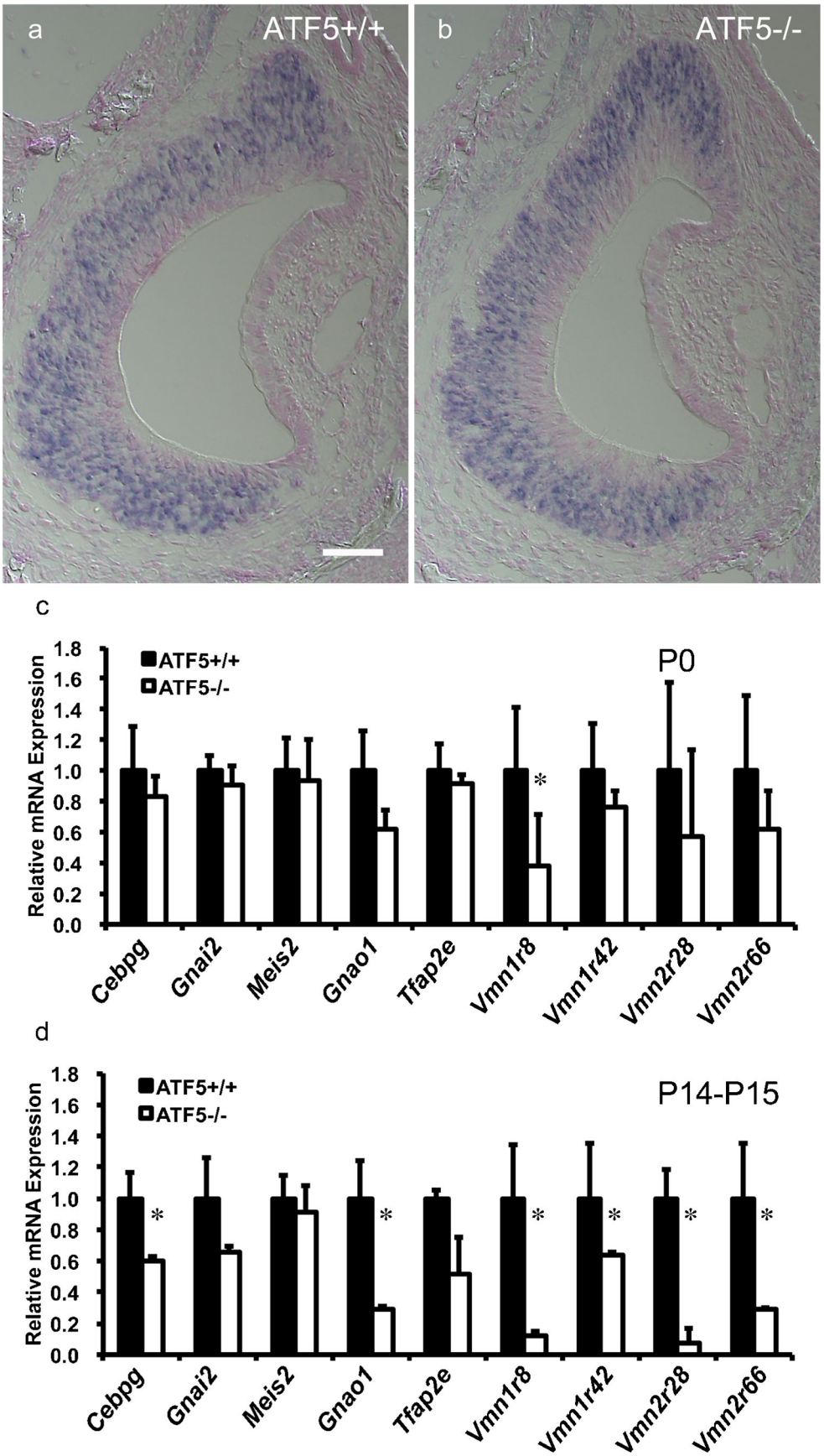
a
ATF5+/+
b
ATF5-/-
c
ATF5+/+
ATF5-/-
P0
Relative mRNA Expression
1.8
1.6
1.4
1.2
1.0
0.8
0.6
0.4
0.2
0.0
*
Cebpg
Gnai2
Meis2
Gnao1
Tfap2e
Vmn1r8
Vmn1r42
Vmn2r28
Vmn2r66
d
ATF5+/+
ATF5-/-
P14-P15
Relative mRNA Expression
1.8
1.6
1.4
1.2
1.0
0.8
0.6
0.4
0.2
0.0
*
Cebpg
Gnai2
Meis2
Gnao1
Tfap2e
Vmn1r8
Vmn1r42
Vmn2r28
Vmn2r66

wild type (Fig. 4d). The expression of *Gnao1* and all vomeronasal receptor genes examined (*Vmn1r8*, *Vmn1r42*, *Vmn2r28*, *Vmn2r66*) was significantly decreased in the ATF5$^{-/-}$ VNO at this stage (Fig. 4d).

The expression of a series of V1r and V2r vomeronasal receptors was significantly decreased in the ATF5$^{-/-}$ VNO (Fig. 4c, d; Nakano et al. 2016), proposing that ATF5 may directly regulate the transcription of V1rs and V2rs. We searched for potential C/EBPγ and ATF5 heterodimer-binding sites (CARE: TGATGCAAT) in the upstream region (2 kb) of 191 V1r and 121 V2r genes using JASPAR software (http://jaspar.genereg.net). We noted that 155 and 99 out of 191 V1rs (81.2%) and 121 V2rs (81.8%), respectively, contained at least one CARE site in the suggested promoter regions (Supplemental Table S1). To confirm whether C/EBPγ and ATF5 regulate V2r transcription, we selected the Vmn2r66 gene containing the predicted CARE with a high score (12.157, Supplemental Table S1); constructed the luciferase reporter plasmid, pVmn2r66-Luc1, containing the promoter region of *Vmn2r66* (approximately 1.4 kb; Fig. 5a); and then tested luciferase activity in Neuro2a cells. As shown in Fig. 5b, the co-expression of C/EBPγ and ATF5 synergistically increased luciferase activity, while the single expression of either had a negligible effect on activity levels. We constructed promoter luciferase reporters with the *Vmn2r28* and *Vmn2r69* genes (pVmn2r28-Luc and pVmn2r69-Luc) that contained the predicted CARE with relatively low (8.50613) and high (11.8258) scores, respectively (Supplemental Table S1), and a promoter luciferase reporter with the *Vmn2r82* gene (pVmn2r82-Luc) that contained no predicted CARE (Supplemental Fig. S3). We found that the co-expression of C/EBPγ and ATF5 induced significant increases of 2- and 5-fold in luciferase activity with pVmn2r28-Luc and pVmn2r69-Luc, respectively, whereas less than a 1.5-fold increase was observed with pVmn2r82-Luc (Supplemental Fig. S3). We then constructed two deletion mutants including pVmn2r66-Luc1 with different promoter region sizes (1.0-kb pVmn2r66-Luc2 and 0.5-kb pVmn2r66-Luc3; Fig. 5a) and found that 0.5 kb of the promoter was sufficient to yield responses (Fig. 5c). We introduced the mutation into the CARE site (TGATGTAATC) with pVmn2r66-Luc4 containing 0.35 kb of the Vmn2r66 promoter and constructed pVmn2r66-Luc4mut (Fig. 5a). We found that luciferase activity induced by the co-expression of C/EBPγ and ATF5 was attenuated with pVmn2r66-Luc4mut (Fig. 5d). These results indicated that C/EBPγ and ATF5 affected the promoter to induce V2r receptor transcription via CARE.

Discussion

In the present study, we investigated the expression and function of the transcription factor C/EBPγ, a heterodimer partner with ATF5, in the mouse VNO. We demonstrated that approximately 70% of the VSN expressed C/EBPγ during the first postnatal week, while 20% of the total VSNs co-expressed C/EBPγ and ATF5 in their nuclei. The co-expression of C/EBPγ and ATF5 activated V2r-promoter-driven reporter gene expression via CARE. The ATF5 deficiency restrains V2r/Gαo-type VSNs at their immature stages and induces apoptotic cell death (Nakano et al. 2016). The present results revealed strong co-expression between C/EBPγ and ATF5 in VSNs, suggesting a role for C/EBPγ in the ATF5-regulated maturation and survival of VSNs in early postnatal development.

The neurogenesis of rodent VSNs in the VNE starts from embryonic day 11 (Cuschieri and Bannister 1975; Suzuki et al. 2003; Enomoto et al. 2011); however, the postnatal development is important for the full organization of the VNE, including the segregation of two major V1r/Gαi2- and V2r/Gαo-type VSN layers in apical and basal VNE, respectively (Berghard and Buck 1996; Jia and Halpern 1996; Herrada and Dulac 1997; Matsunami and Buck 1997; Ryba and Tirindelli 1997; Enomoto et al. 2011; Prince et al. 2013), in addition to the localization of mature VSNs in the central region and proliferating cells and immature VSNs in the marginal region of the VNE (Barber and Raisman 1978; Giacobini et al. 2000; Martinez-Marcos et al. 2005; Brann and Firestein 2010; de la Rosa-Prieto et al. 2010; Oboti et al. 2015). In the present study, we demonstrated that *C/EBPγ* mRNA was broadly expressed in the VSNs of the VNE in the neonatal stage, and its expression was decreased and localized in the

Fig. 5 Upregulation of *Vmn2r66* promoter activity by the co-expression of C/EBPγ and ATF5. **a** Schematic representation of Vmn2r66 promoter luciferase reporter constructs. The Vmn2r66 promoter region (approximately 1.4 kb) was cloned upstream of the firefly luciferase coding region of the pGL3 vector to produce pVmn2r66-Luc1, creating three different 5′ region deletion constructs (pVmn2r66-Luc2, pVmn2r66-Luc3, and pVmn2r66-Luc4). A mutation was introduced into the CARE site (shown by the square) in pVmn2r66-Luc4 to produce pVmn2r66-Luc4mut. **b** Neuro2a cells in 24-well formats were transfected with pVmn2r66-Luc1 and either C/EBPγ, ATF5, or C/EBPγ+ATF5 expression vectors (pcDNA, total 200 ng/well). The plasmid pRL-SV40 expressing *Renilla* luciferase was included as the loading control for transfection efficiency. Reporter luciferase activities were normalized to each *Renilla* luciferase activity and expressed as relative values against the parental vector (pcDNA). Data are the average ± SD calculated from the results of triplicates from one of three independent experiments. A one-way ANOVA followed by the Tukey-Kramer test was performed (different letters indicate a significant difference, $P < 0.05$). **c** Effects of the deletion with the Vmn2r66 promoter region on C/EBPγ and ATF5-induced luciferase activities in Neuro2a cells. **d** Effects of a mutation with the CARE of the Vmn2r66 promoter region on C/EBPγ and ATF5-induced luciferase activities in Neuro2a cells. Reporter luciferase activities were normalized to each *Renilla* luciferase activity and expressed as relative values against the parental vector (pcDNA). Data are the average ± SD calculated from the results of triplicates from one of two independent experiments. The Student's unpaired *t* test was performed to compare pcDNA and C/EBPγ+ATF5 (*$P < 0.05$)

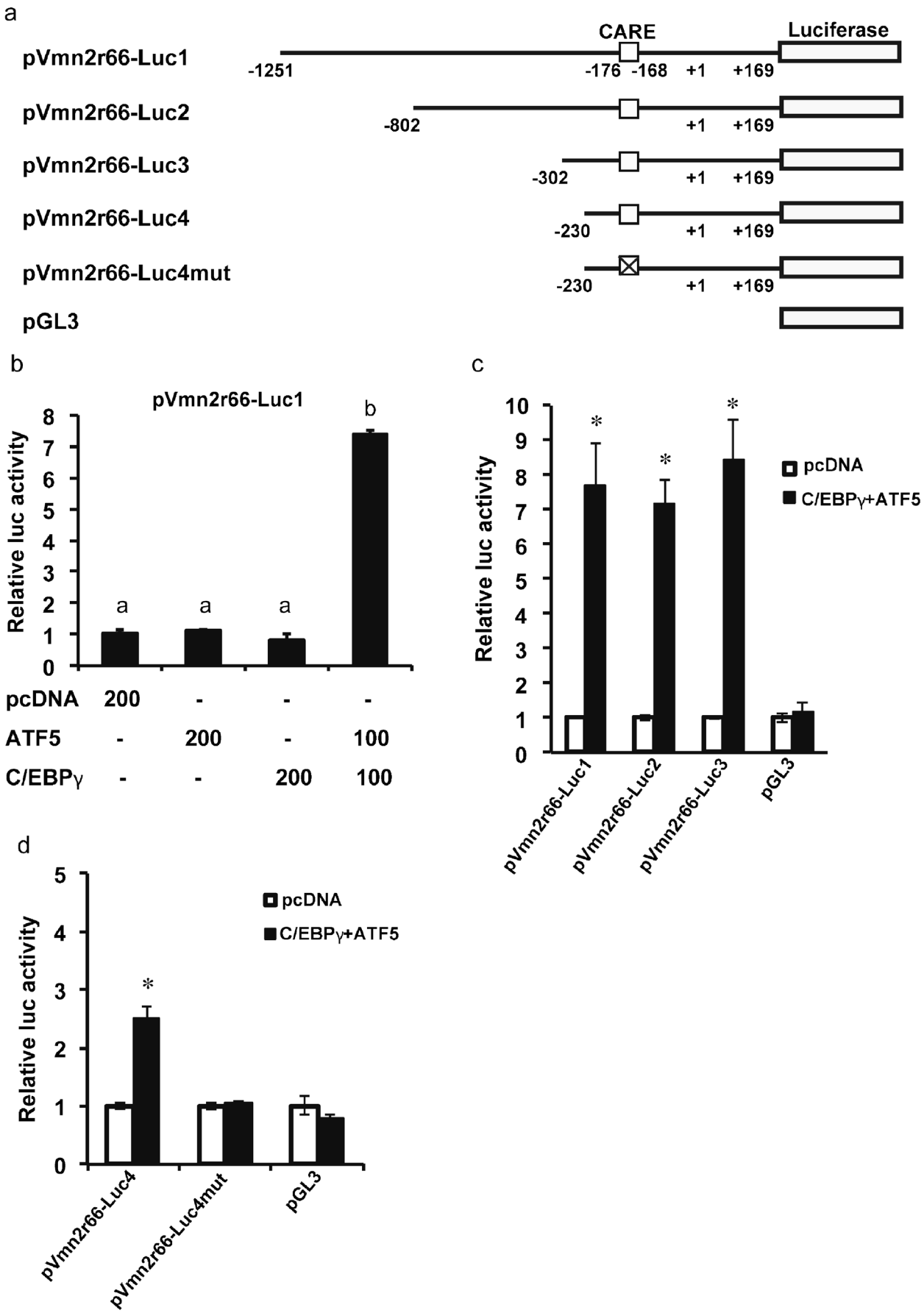
a
CARE
Luciferase
pVmn2r66-Luc1
-1251
-176 -168 +1 +169
pVmn2r66-Luc2
-802
+1 +169
pVmn2r66-Luc3
-302
+1 +169
pVmn2r66-Luc4
-230
+1 +169
pVmn2r66-Luc4mut
-230
+1 +169
pGL3
b
pVmn2r66-Luc1
Relative luc activity
a a a b
pcDNA 200 - - -
ATF5 - 200 - 100
C/EBPγ - - 200 100
c
Relative luc activity
pcDNA
C/EBPγ+ATF5
pVmn2r66-Luc1
pVmn2r66-Luc2
pVmn2r66-Luc3
pGL3
d
Relative luc activity
pcDNA
C/EBPγ+ATF5
pVmn2r66-Luc4
pVmn2r66-Luc4mut
pGL3

marginal region of the VNE by P15. The expression pattern was similar to that of *Bcl11b*, a transcription factor that is critical for VSN differentiation (Enomoto et al. 2011). *C/EBPγ* mRNA signals in the marginal region overlapped with *GAP43* (partially with *OMP*) and co-labeled with both *Gαi2* and *Gαo*, indicating that *C/EBPγ*-expressing cells corresponded to immature and some mature V1r/Gαi2- and V2r/Gαo-type VSNs. The co-localization of *C/EBPγ* and *GAP43* was also observed in olfactory sensory neurons (OSNs) of the MOE (Supplemental Fig. S1), indicating *C/EBPγ* was a common immature neuron marker in both OSNs and VSNs. At the protein level, more than 90% of C/EBPγ-positive VSNs were labeled with DCX (immature and early mature marker) from P0 to P21, and the co-labeled VSNs with OMP increased from 30% at P0 to more than 80% of C/EBPγ-positive cells at P7 and, thereafter, supporting C/EBPγ being strongly expressed in the immature and early mature stages of VSNs.

Double immunofluorescence revealed that C/EBPγ and ATF5 proteins were co-expressed in the nuclei of 20% of the VSNs for the first postnatal week, and these co-expressed cells decreased to approximately 2% of the VSNs at P15 and, thereafter, indicating that the role of C/EBPγ and ATF5 is primarily limited to the earliest postnatal stages. Neonatal VSNs achieve the full development of endoplasmic reticulum (ER) in the cytoplasm by the end of the first postnatal week (Garrosa and Coca 1991). The ATF5 translation is facilitated by ER stress response with Perk-mediated eIF2α phosphorylation in various cell types, including OSNs and VSNs (Watatani et al. 2008; Zhou et al. 2008; Dalton et al. 2013; Hatano et al. 2013; Dalton 2018). In OSNs, olfactory receptor (OR) expression triggers ER stress response and activates ATF5 translation, resulting in the maturation of OSNs with stable expression of the selected OR (Dalton et al. 2013). We speculate that the active synthesis of vomeronasal receptors and axon guidance molecules might cause ER stress and enhance ATF5 translation in VSNs at the maturation phase. Our results with the C/EBPγ expression in immature and mature VSNs and the impaired maturation in ATF5-deficient VSNs (Nakano et al. 2016) suggest the role of C/EBPγ and ATF5 to drive the maturation of VSNs. The reduction of VSNs co-expressed with C/EBPγ and ATF5 at the later postnatal stages (P15–P32) might be due to the decrease of proliferating cells that supply early postmitotic VSNs since proliferating cells are broadly distributed throughout the neonatal VNE but drastically decrease and localized to the marginal region of the VNE at P10 and thereafter (Weiler et al. 1999; Wakabayashi and Ichikawa 2007). Proliferating cells can be stimulated in regenerative VNO by the lesion of vomeronasal nerves (Brann and Firestein 2010), which may give rise to C/EBPγ and ATF5-expressing VSNs in the adult VNE. Transcription factors other than C/EBPγ and ATF5 are likely to play a role to generate mature VSNs at later postnatal stages since the VSN neurogenesis continues in the adult VNE (Barber and Raisman 1978; Giacobini et al. 2000; Martinez-Marcos et al. 2005; Brann and Firestein 2010; de la Rosa-Prieto et al. 2010; Oboti et al. 2015). Transcription factors Meis2 and Tfap2e are exclusively expressed in apical and basal VSNs, respectively (Enomoto et al. 2011; Chang and Parrilla 2016) for at least postnatal 3 weeks (Chang and Parrilla 2016). Tfap2e-deficient mice have recently revealed that Tfap2e is critical for basal VSNs differentiation and V2r expression (Lin et al. 2018).

C/EBPγ did not appear to be a transcriptional target of ATF5 because C/EBPγ mRNA expression in $ATF5^{-/-}$ VNO was similar to that in $ATF5^{+/+}$ VNO at P0. We observed a significant decrease in C/EBPγ mRNA in $ATF5^{-/-}$ VNO at P15 (Fig. 4d). Considering both V1r/Gαi2- and V2r/Gαo-type VSNs expressed C/EBPγ mRNAs (Fig. 1m, n), the decrease in C/EBPγ in $ATF5^{-/-}$ VNO appeared to be due to the loss of basal VSNs because the expression of Gαo (Gnao1) but not Gαi2 (Gnai2) mRNA was significantly reduced (Fig. 4d).

Since the ATF5 deficiency causes the decreased expression of V1r and V2r genes in the VNE (Fig. 4c, d; Nakano et al. 2016), we hypothesized that C/EBPγ and ATF5 may regulate V1r and V2r expression in VSNs. Our promoter reporter assay results provide an insight into the potential role of C/EBPγ and ATF5 in the transcription of some V2r genes via cis-regulatory CARE. The co-regulation of C/EBPγ and ATF4 on many stress responsive genes in the reactive oxygen species (ROS) pathway via CARE has recently been reported (Huggins et al. 2016), supporting the importance of CARE with C/EBPγ and ATF5 for V2r promoter activity. The ATF5 deficiency is shown to promote the apoptosis of β cells as well as VSNs (Nakano et al. 2016; Juliana et al. 2017). ATF5 directly regulates the transcription of eIF4E-binding protein 1 (4EBP1) via upstream CARE binding and thereby prevents β cells from overloading proteins in ER (Juliana et al. 2017). C/EBPγ and ATF5 may also target genes that function in cell survival and apoptosis in VSNs. Further studies using C/EBPγ-deficient mice will contribute to clarifying the function of C/EBPγ in the development of the vomeronasal system. C/EBPγ-deficient mice die perinatally and exhibit atelectasis of the lung (Kaisho et al. 1999: Huggins et al. 2016). A deficiency in C/EBPγ has been shown to reduce the cytolytic activity of natural killer (NK) cells (Kaisho et al. 1999) and induce abnormal lens formation (Huggins et al. 2016).

In conclusion, we herein demonstrated the co-expression of C/EBPγ and ATF5 in differentiating VSNs of the postnatal VNO and their cooperative effects on V2r promoter activation, suggesting a potential role for C/EBPγ in ATF5-driven VSN differentiation. C/EBPγ was expressed in immature and early mature VSNs but lacked a transactivation domain, and, thus, the transient co-expression with ATF5 translated by ER stress response may provide a critical period for VSNs to reach maturity and survive.

Acknowledgments We thank the members of the Takahashi laboratory for their support and useful discussions.

Compliance with ethical standards All mouse studies were approved by the Institutional Animal Experiment Committee of the university and were performed in accordance with institutional and governmental guidelines.

References

Barber PC, Raisman G (1978) Cell division in the vomeronasal organ of the adult mouse. Brain Res 141:57–66

Berghard A, Buck LB (1996) Sensory transduction in vomeronasal neurons: evidence for G alpha o, G alpha i2, and adenylyl cyclase II as major components of a pheromone signaling cascade. J Neurosci 16: 909–918

Brann JH, Firestein S (2010) Regeneration of new neurons is preserved in aged vomeronasal epithelia. J Neurosci 30:15686–15694

Cau E, Gradwohl G, Fode C, Guillemot F (1997) Mash1 activates a cascade of bHLH regulators in olfactory neuron progenitors. Development 124:1611–1621

Chang I, Parrilla M (2016) Expression patterns of homeobox genes in the mouse vomeronasal organ at postnatal stages. Gene Expr Patterns 21:69–80

Cooper C, Henderson A, Artandi S, Avitahl N, Calame K (1995) Ig/EBP (C/EBPγ) is a transdominant negative inhibitor of C/EBP family transcriptional activators. Nucleic Acids Res 23:4371–4377

Cuschieri A, Bannister LH (1975) The development of the olfactory mucosa in the mouse: light microscopy. J Anat 119:277–286

Dalton RP (2018) Shared genetic requirements for ATF5 translation in the vomeronasal organ and main olfactory epithelium [version 1; referees: awaiting peer review]. F1000Research 7:73. https://doi.org/10.12688/f1000research.13659.1)

Dalton RP, Lyons DB, Lomvardas S (2013) Co-opting the unfolded protein response to elicit olfactory receptor feedback. Cell 155:321–332

De La Rosa-Prieto C, Saiz-Sanchez D, Ubeda-Banon I, Argandona-Palacios L, Garcia-Munozguren S, Martinez-Marcos A (2010) Neurogenesis in subclasses of vomeronasal sensory neurons in adult mice. Dev Neurobiol 70:961–970

Dulac C, Axel R (1995) A novel family of genes encoding putative pheromone receptors in mammals. Cell 83:195–206

Enomoto T, Ohmoto M, Iwata T, Uno A, Saitou M, Yamaguchi T, Kominami R, Matsumoto I, Hirota J (2011) Bcl11b/Ctip2 controls the differentiation of vomeronasal sensory neurons in mice. J Neurosci 31:10159–10173

Garrosa M, Coca S (1991) Postnatal development of the vomeronasal epithelium in rat: an ultrastructural study. J Morphol 208:257–269

Giacobini P, Benedetto A, Tirindelli R, Fasolo A (2000) Proliferation and migration of receptor neurons in the vomeronasal organ of the adult mouse. Dev Brain Res 123:33–40

Hatano M, Umemura M, Kimura N, Yamazaki T, Takeda H, Nakano H, Takahashi S, Takahashi Y (2013) The 5′-untranslated region regulates ATF5 mRNA stability via nonsense-mediated mRNA decay in response to environmental stress. FEBS J 280:4693–4707

Herrada G, Dulac C (1997) A novel family of putative pheromone receptors in mammals with a topographically organized and sexually dimorphic distribution. Cell 90:763–773

Huggins CJ, Mayekar MK, Martin N, Saylor KL, Gonit M, Jailwala P, Kasoji M, Haines DC, Quinones OA, Johnson PF (2016) C/EBPγ is a critical regulator of cellular stress response networks through heterodimerization with ATF4. Mol Cell Biol 36:693–713

Ibarra-Soria X, Levitin MO, Saraiva LR, Logan DW (2014) The olfactory transcriptomes of mice. PLoS Genet 10:e1004593

Jia C, Halpern M (1996) Subclasses of vomeronasal receptor neurons: differential expression of G proteins (Gi alpha 2 and G(o alpha)) and segregated projections to the accessory olfactory bulb. Brain Res 719:117–128

Juliana CA, Yang J, Rozo AV, Good A, Groff DN, Wang SZ, Green MR, Stoffers DA (2017) ATF5 regulates β-cell survival during stress. Proc Natl Acad Sci U S A 114:1341–1346

Kaisho T, Tsutsui H, Tanaka T, Tsujimura T, Takeda K, Kawai T, Yoshida N, Nakanishi K, Akira S (1999) Impairment of natural killer cytotoxic activity and interferon gamma production in CCAAT/enhancer binding protein gamma-deficient mice. J Exp Med 190:1573–1582

Khan A, Fornes O, Stigliani A, Gheorghe M, Castro-Mondragon JA, van der Lee R, Bessy A, Cheneby J, Kulkarni SR, Tan G, Baranasic D, Arenillas DJ, Sandelin A, Vandepoele K, Lenhard B, Ballester B, Wasserman WW, Parcy F, Mathelier A (2018) JASPAR 2018: update of the open-access database of transcription factor binding profiles and its web framework. Nucleic Acids Res 46:D260–D266

Liberles SD (2014) Mammalian pheromones. Annu Rev Physiol 76:151–175

Lin JM, Taroc EZM, Frias JA, Prasad A, Catizone AN, Sammons MA, Forni PE (2018) The transcription factor Tfap2e/AP-2ε plays a pivotal role in maintaining the identity of basal vomeronasal sensory neurons. Dev Biol 441:67–82

Martinez-Marcos A, Jia C, Quan W, Halpern M (2005) Neurogenesis, migration, and apoptosis in the vomeronasal epithelium of adult mice. J Neurobiol 63:173–187

Matsunami H, Buck LB (1997) A multigene family encoding a diverse array of putative pheromone receptors in mammals. Cell 90:775–784

Murray RC, Navi D, Fesenko J, Lander AD, Calof AL (2003) Widespread defects in the primary olfactory pathway caused by loss of Mash1 function. J Neurosci 23:1769–1780

Nakano H, Iida Y, Suzuki M, Aoki M, Umemura M, Takahashi S, Takahashi Y (2016) Activating transcription factor 5 (ATF5) is essential for the maturation and survival of mouse basal vomeronasal sensory neurons. Cell Tissue Res 363:621–633

Newman JR, Keating AE (2003) Comprehensive identification of human bZIP interactions with coiled-coil arrays. Science 300:2097–2101

Nishizawa M, Nagata S (1992) cDNA clones encoding leucine-zipper proteins which interact with G-CSF gene promoter element 1-binding protein. FEBS Lett 299:36–38

Oboti L, Ibarra-Soria X, Perez-Gomez A, Schmid A, Pyrski M, Paschek N, Kircher S, Logan DW, Leinders-Zufall T, Zufall F, Chamero P (2015) Pregnancy and estrogen enhance neural progenitor-cell proliferation in the vomeronasal sensory epithelium. BMC Biol 13:104

Prince JE, Brignall AC, Cutforth T, Shen K, Cloutier JF (2013) Kirrel3 is required for the coalescence of vomeronasal sensory neuron axons into glomeruli and for male-male aggression. Development 140: 2398–2408

Ryba NJ, Tirindelli R (1997) A new multigene family of putative pheromone receptors. Neuron 19:371–379

Shimizu YI, Morita M, Ohmi A, Aoyagi S, Ebihara H, Tonaki D, Horino Y, Iijima M, Hirose H, Takahashi S, Takahashi Y (2009) Fasting induced up-regulation of activating transcription factor 5 in mouse liver. Life Sci 84:894–902

Simmons DG, Natale DR, Begay V, Hughes M, Leutz A, Cross JC (2008) Early patterning of the chorion leads to the trilaminar trophoblast cell structure in the placental labyrinth. Development 135:2083–2091

Suzuki Y, Mizoguchi I, Nishiyama H, Takeda M, Obara N (2003) Expression of Hes6 and NeuroD in the olfactory epithelium, vomeronasal organ and non-sensory patches. Chem Senses 28: 197–205

Umemura M, Tsunematsu K, Shimizu YI, Nakano H, Takahashi S, Higashiura Y, Okabe M, Takahashi Y (2015) Activating

transcription factor 5 is required for mouse olfactory bulb development via interneuron. Biosci Biotechnol Biochem 79:1082–1089

Vinson CR, Hai T, Boyd SM (1993) Dimerization specificity of the leucine zipper-containing bZIP motif on DNA binding: prediction and rational design. Genes Dev 7:1047–1058

Wakabayashi Y, Ichikawa M (2007) Distribution of Notch1-expressing cells and proliferating cells in mouse vomeronasal organ. Neurosci Lett 411:217–221

Wang SZ, Ou J, Zhu LJ, Green MR (2012) Transcription factor ATF5 is required for terminal differentiation and survival of olfactory sensory neurons. Proc Natl Acad Sci U S A 109:18589–18594

Watatani Y, Ichikawa K, Nakanishi N, Fujimoto M, Takeda H, Kimura N, Hirose H, Takahashi S, Takahashi Y (2008) Stress-induced translation of ATF5 mRNA is regulated by the 5′-untranslated region. J Biol Chem 283:2543–2553

Weiler E, McCulloch MA, Farbman AI (1999) Proliferation in the vomeronasal organ of the rat during postnatal development. Eur J Neurosci 11:700–711

Zhao Y, Zhang YD, Zhang YY, Qian SW, Zhang ZC, Li SF, Guo L, Liu Y, Wen B, Lei QY, Tang QQ, Li X (2014) p300-dependent acetylation of activating transcription factor 5 enhances C/EBPβ transactivation of C/EBPα during 3T3-L1 differentiation. Mol Cell Biol 34:315–324

Zhou D, Palam LR, Jiang L, Narasimhan J, Staschke KA, Wek RC (2008) Phosphorylation of eIF2 directs ATF5 translational control in response to diverse stress conditions. J Biol Chem 283:7064–7073